The Astrophysical Journal Letters, 935:L36 (4pp), 2022 August 20 https://doi.org/10.3847/2041-8213/ac88bf


# Discovery of γ-Ray Pulsations from PSR J1835–3259B in the Globular Cluster NGC 6652

Pengfei Zhang[1], Yi Xing[2], and Zhongxiang Wang[1,2]
[1] Department of Astronomy, School of Physics and Astronomy, Key Laboratory of Astroparticle Physics of Yunnan Province, Yunnan University, Kunming 650091, People's Republic of China; zhangpengfei@ynu.edu.cn, wangzx20@ynu.edu.cn
[2] Key Laboratory for Research in Galaxies and Cosmology, Shanghai Astronomical Observatory, Chinese Academy of Sciences, 80 Nandan Road, Shanghai 200030, People's Republic of China; yixing@shao.ac.cn
*Received 2022 June 24; revised 2022 August 7; accepted 2022 August 10; published 2022 August 23*

## Abstract

Motivated by the recent discovery of the pulsar J1835−3259B with a spin period 1.83 ms in the globular cluster (GC) NGC 6652, we analyze the γ-ray data obtained with the Large Area Telescope on board the Fermi Gamma-ray Space Telescope (Fermi) for the GC and detect the pulsations of this millisecond pulsar (MSP) at a $5.4\sigma$ confidence level (the weighted H-test value is ∼41). From timing analysis of the data, a pulse profile that is similar to the radio one is established. We thus consider that we have detected the γ-ray emission of the MSP, and discuss the implications. Based on the results of our analysis and different studies of the sources in the GC, the observed γ-ray emission from the GC could mainly arise from this MSP, like the previous two cases in the GCs NGC 6624 and NGC 6626. Assuming this is the case, the pulsar, at the GC's distance of 9.46 kpc and having a spin-down luminosity of $\leqslant 4.3 \times 10^{35}$ erg s$^{-1}$, would have a γ-ray luminosity of $\simeq (5.04 \pm 0.44) \times 10^{34}$ erg s$^{-1}$ and a γ-ray efficiency of $\gtrsim 0.12$.

*Unified Astronomy Thesaurus concepts:* Gamma-rays (637); Globular star clusters (656); Pulsars (1306)

## 1. Introduction

Globular clusters (GCs) are spherical ensembles of old stars that constitute as an important part of our Galaxy. They each contain $\sim 10^5$ stars, and most have typical ages of greater than $10^{10}$ yr (e.g., Harris 1996). Owing to the high stellar densities and thus frequent dynamical interactions in their cores, GCs are the natural sites to form compact low-mass X-ray binaries, whose further evolution resulting in the formation of millisecond pulsars (MSPs; Bhattacharya & van den Heuvel 1991). Therefore GCs can be considered as factories of MSPs. This scenario is supported by the observational facts that thus far 257 MSPs have been detected in 36 GCs within ∼20 kpc of the Galactic center[3] and these GC MSPs constitute ∼50% of known MSPs in our Galaxy (Manchester et al. 2005).

Since the successful launch of the Fermi Gamma-ray Space Telescope (Fermi) and use of the Large Area Telescope (LAT) on board (Atwood et al. 2009), the first detection of γ-rays from a GCs, 47 Tuc, was reported by Abdo et al. (2009), which was followed by that of Terzan 5 by Kong et al. (2010). Approximately 40 GCs have now been reported to have detectable γ-ray emission (Abdo et al. 2010a, 2010b; Tam et al. 2011; Zhou et al. 2015; Zhang et al. 2016; Lloyd et al. 2018; de Menezes et al. 2019; Abdollahi et al. 2020; Yuan et al. 2022). It is generally considered that the γ-ray emission from GCs primarily arises from the MSPs contained within them. This consideration has been well supported by the discoveries of pulsed γ-ray emission from an individual pulsar that dominates the γ-ray emission detected from a whole GC, specifically PSR J1823−3021A in NGC 6624 (Freire et al. 2011) and B1821−24 in NGC 6626 (or M28; Wu et al. 2013; Johnson et al. 2013). Also, not only the γ-ray luminosities of the GCs but also their γ-ray spectra have been analyzed to show that the emission is consistent with that arising from a number of MSPs in each GC (Abdo et al. 2010a; Hui et al. 2011; Lloyd et al. 2018; de Menezes et al. 2019; Zhang et al. 2020; Song et al. 2021; Wu et al. 2022).

Recently, Gautam et al. (2022) reported the discovery of a 1.83 ms MSP, PSR J1835−3259B, in a near-circular orbit of 28.7 hr within the GC NGC 6652. This MSP is the second one found in this GC; the first is PSR J1835−3259A, which has a spin period of 3.89 ms and is in a wide binary with orbital period 9.25 days (DeCesar et al. 2015). NGC 6652 also shows detectable γ-ray emission, with counterparts named J1835.3−3255 in the first Fermi-LAT source catalog (1FGL; Abdo et al. 2010a) and J1835.7−3258 in the fourth catalog (4FGL; Fermi-LAT Collaboration et al. 2022). Based on its γ-ray spectrum and using a source distance of 10 kpc (Harris 1996), Wu et al. (2022) estimated that this GC contains 1–7 MSPs. Motivated by these results and given the detailed ephemeris for PSR J1835−3259B provided in Gautam et al. (2022), we carried out timing analysis of the Fermi-LAT data for NGC 6652. We have been able to detect γ-ray pulsations from PSR J1835−3259B. Here we report the analysis and results.

## 2. Analysis and Results

### 2.1. Fermi-LAT Data and Source Model

We selected the Fermi-LAT Pass 8 *FrontBack* events (evclass = 128 and evtype = 3) in the energy range 0.1–500.0 GeV within a 20° × 20° region of interest centered on NGC 6652 (R.A. = $18^h35^m45\overset{s}{.}502$, decl. = −32°58′15.″621). The time range of the data was from 2008 August 4 16:29:16.8 to 2022 June 15 22:12:11.0 (UTC). We excluded events with zenith angles >90° to avoid contamination from the Earth's limb and those with quality flags of "bad" (judged

[3] http://www.naic.edu/~pfreire/GCpsr.html

**Table 1**
Likelihood Analysis Results

| Models | Parameter Values | | |
|---|---|---|---|
| LP | $\alpha$ | $\beta$ | $E_b$ (GeV) |
| | 2.051(98) | 0.400(69) | 1.158(45) |
| | 2.23(12)[a] | 0.29(09)[a] | 1.16[a] |
| PLEC | $\Gamma$ | $b$ | $E_c$ (GeV) |
| | 1.544(95) | 1.01(14) | 3.00(33) |

**Note.**
[a] 4FGL-DR3 values for the LP model; no errors (numbers in parentheses) were given for $E_b$.

by the expression DATA_QUAL > 0 && LAT_CONFIG = 1), and the instrumental response function "P8R3 SOURCE V3" was used. Thus high-quality data in good time intervals were selected. The package Fermitools–2.0.19 was used in the analysis.

Based on Data Release 3 of 4FGL (4FGL-DR3; Fermi-LAT Collaboration et al. 2022), which was constructed from 12 years of LAT data, a model file was made with the script make4FGLxml.py.[4] The model file included the spectral parameters of the catalog sources within 25° of NGC 6652, and their spectral forms provided in 4FGL-DR3 were used. We set free the parameters of flux normalizations and spectral shapes for the sources within 5°. Other free parameters included the normalizations of the sources within 5°−10°, those outside 10° but identified with *Variablility_Index* ⩾ 72.44 (i.e., variable sources), and the Galactic and extragalactic diffuse emission components. All other parameters were fixed at their values provided in 4FGL-DR3.

### 2.2. Data Analysis and Spectrum Extraction

A binned maximum likelihood analysis was performed on the whole LAT data set, where the log-parabola (LP) model provided in 4FGL-DR3 for NGC 6652, $dN/dE = N_0(E/E_b)^{-[\alpha+\beta\log(E/E_b)]}$, was used. The obtained best-fit parameter values are given in Table 1 and are in agreement with those given in 4FGL-DR3. The corresponding flux in 0.1–500.0 GeV was $(4.07 \pm 0.74) \times 10^{-9}$ photons cm$^{-2}$ s$^{-1}$ and the test statistic (TS) value was ≃212. Because we consider that the γ-ray emission likely arises from the MSPs, we then used the model of a power law with an exponential cutoff (PLEC), $dN/dE = N_0(E/E_0)^{-\Gamma}\exp[-(E/E_c)^b]$, which is typical for describing pulsars' γ-ray emission. Performing the likelihood analysis, the best-fit parameter values were obtained and are given in Table 1. The corresponding flux in 0.1–500 GeV was $(5.71 \pm 0.84) \times 10^{-9}$ photons cm$^{-2}$ s$^{-1}$ and the TS value was ∼208. As this TS value is only slightly smaller than that from the LP model, the two models (shown in Figure 1) should be considered equally good for fitting the γ-ray emission of NGC 6652. A new parameterization was developed for fitting emission from pulsars in 4FGL-DR3, so we tested the model, PLEC4 (see Fermi-LAT Collaboration et al. 2022 for details), and the results were similar to those from PLEC (see Figure 1).

We adopted the PLEC model in the following analysis, and the obtained best-fit parameters were saved in the source model. Using the best-fit parameters of the PLEC, the integrated energy flux was calculated to be $(4.71 \pm 0.39) \times 10^{-12}$ erg cm$^{-2}$ s$^{-1}$, and considering the newly reported source distance 9.46 ± 0.14 kpc for the GC (Baumgardt & Vasiliev 2021), the γ-ray luminosity (assuming isotropic emission) is $L_\gamma = (5.04 \pm 0.44) \times 10^{34}$ erg s$^{-1}$.

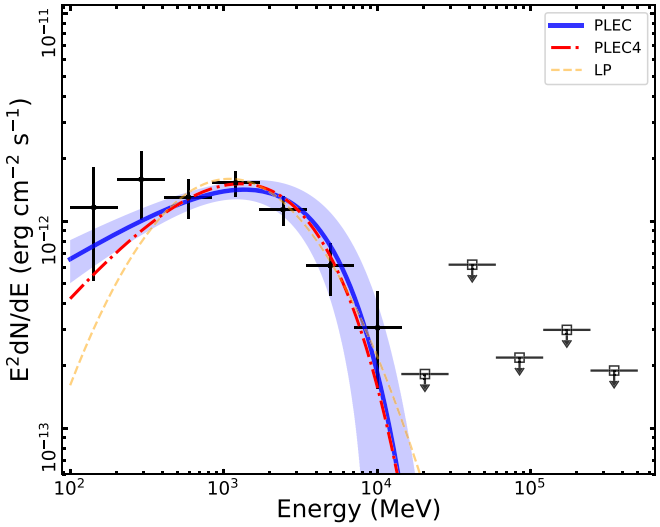


**Figure 1.** γ-ray spectrum at 0.1–500 GeV obtained from the data for NGC 6652. The best-fit LP and PLEC models are shown as yellow dashed and blue solid lines respectively. The error range of the latter is also shown as the light blue region. A testing PLEC4 model is shown as the red dashed–dotted line (see Section 2.2).

Based on the updated source model, in which the parameters of spectral shapes for all the sources were fixed at their best-fit values obtained above and the normalizations of the sources within 10° of the target and the two background components were set as free parameters, we performed spectral analysis. The 0.1–500.0 GeV energy range was divided into 12 equally logarithmically spaced energy bins. A spectrum of the whole LAT data set was extracted by performing the maximum likelihood analysis on the data in each energy bin. The obtained spectrum is shown in Figure 1, for which we kept the flux data points with TS values ⩾4 and showed 95% flux upper limits otherwise. This spectrum is relatively well described by the PLEC model, whose Γ is within and $E_c$ is slightly higher than the respective ranges determined from the spectra of 104 γ-ray MSPs (Wu et al. 2022).

### 2.3. Timing Analysis

We selected the events within an aperture radius of 6° (the 68% containment angle at 0.1 GeV[5]) in the 0.1–500 GeV band, and assigned weights to them with their probabilities of originating from the target (using the Fermi tool `gtsrcprob`). Pulse phases were assigned to the weighted photons based on the given ephemeris (Gautam et al. 2022) by employing Tempo2 (Hobbs et al. 2006) with the Fermi plug-in (Ray et al. 2011). The two-dimensional phaseogram and folded pulse profile in 16 phase bins are plotted in Figures 2(B) and (A) respectively, where the uncertainties of the counts in each bin were estimated using the method provided in Abdo et al. (2013). The pulse profile shows a peak at phase ∼0.31–0.44, because the results of the photons with large weights (high probabilities) are mostly located within the phase range

[4] https://fermi.gsfc.nasa.gov/ssc/data/analysis/user/

[5] https://www.slac.stanford.edu/exp/glast/groups/canda/lat_Performance.htm

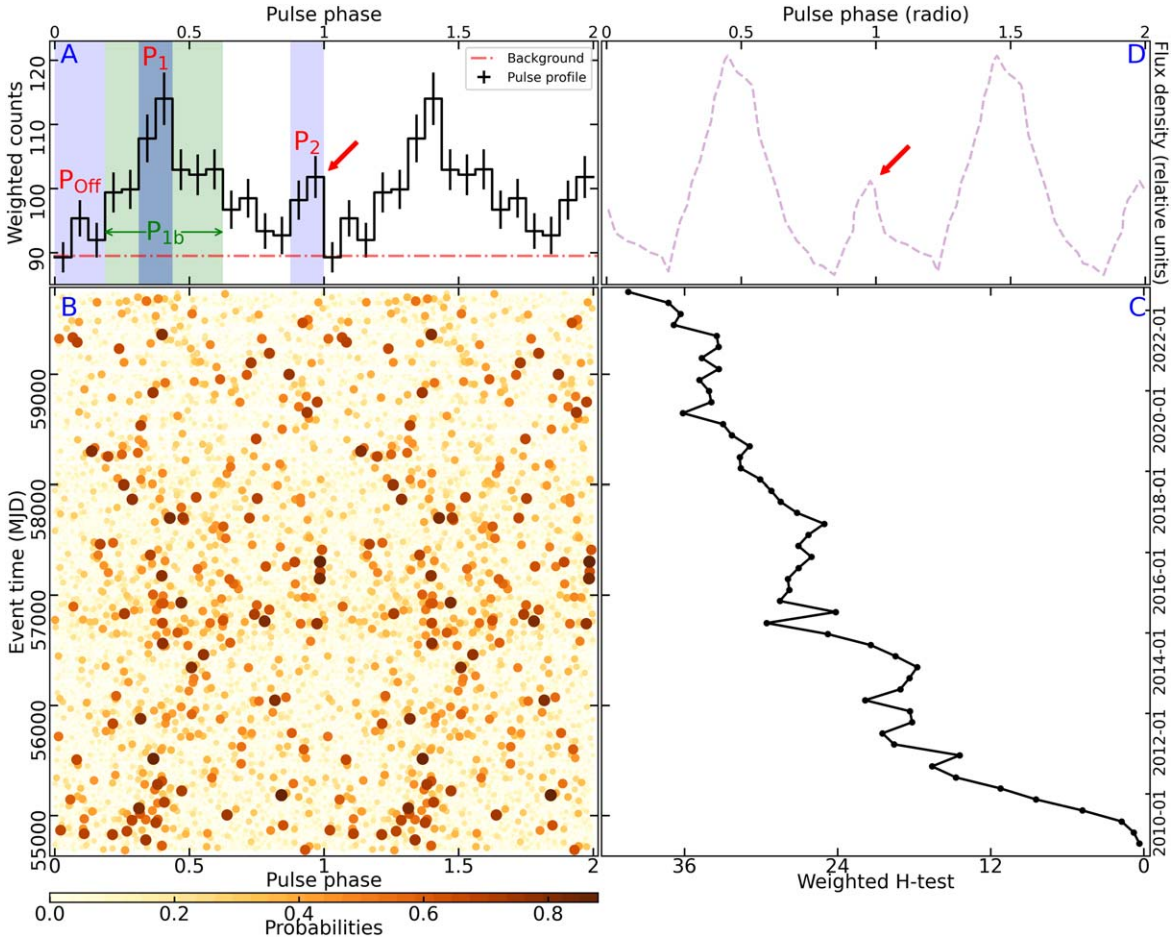


**Figure 2.** Timing analysis results for PSR J1835−3259B. (A) The integrated weighted $\gamma$-ray pulse profile (16 phase bins). (B) Two-dimensional phaseogram (16 phase bins), where the bottom color bar indicates the weights of the photons (with the largest being 88%). (C) H-test values over the span of the data. (D) Schematic radio pulse profile of PSR J1835−3259B drawn from that reported in Gautam et al. (2022) for comparison. Red arrows indicate the mini-peak seen in both $\gamma$-rays and radio.

0.3–0.5, and also a mini-peak at phase ∼0.94–1.0. A great similarity to the shape of the radio pulse profile (Figure 2(D), which was drawn approximately based on that reported in Gautam et al. 2022) is thus seen. Following Abdo et al. (2013), we estimated the background counts (diffuse emission plus contributions from the nearby sources), and the value was 89.5, equal to the lowest one ($89.3 \pm 2.4$) of the pulse bins.

We applied the H-test statistic to the weighted photons (de Jager & Büsching 2010; Kerr 2011), and the curve of cumulative H-test value over the time span of the LAT data is shown in Figure 2(C). The H-test value of the whole data was ≃41, corresponding to a $p$-value of $7.5 \times 10^{-8}$ (≃5.4$\sigma$).

### 2.4. Phase-resolved Analysis

Given the established pulse profile, we first performed the likelihood analysis on the data of the $P_1$ and $P_2$ phase ranges shown in Figure 2(A), for further investigation of the emissions of the pulse peaks. Using the PLEC model, the fits to the main pulse peak ($P_1$) and the mini-peak ($P_2$) were obtained. The best-fit parameters are consistent with those obtained from the whole data set but with large uncertainty ranges, since the TS values were ≃119 and ≃33 respectively.

We also analyzed the data in the $P_{1b}$ and $P_{off}$ phase ranges (Figure 2(A)) to checking the contributions of the major pulsed emission and the possible off-pulse emission respectively. Likelihood analysis resulted in TS values of 189 and 1 respectively. The flux upper limit (95%) for the latter was $\simeq 6.0 \times 10^{-10}$ photons cm$^{-2}$ s$^{-1}$ (or $\sim 5.3 \times 10^{33}$ erg s$^{-1}$ at the GC's distance and assuming the PLEC parameters of the MSP).

## 3. Discussion

By using the ephemeris given by the radio detection of PSR J1835−3259B, we have analyzed the Fermi-LAT data collected for NGC 6652 over approximately 14 years and detected the pulsations of this newly discovered MSP at a 5.4$\sigma$ confidence level. The great similarity of the $\gamma$-ray pulse profile to the radio one also strongly supports our detection. This pulsar has a maximum spin-down rate $\dot{P}$ of $6.65 \times 10^{-20}$ (Gautam et al. 2022), which implies a spin-down luminosity of $\dot{E} \leqslant 4.3 \times 10^{35}$ erg s$^{-1}$. The $\gamma$-ray efficiency would be $\eta = L_\gamma/\dot{E} \gtrsim 0.12$ when we assign the observed $L_\gamma$ to the MSP. The $\eta$ value is in line with those of other MSPs (e.g., Wu et al. 2022), again supporting the detection.

Wu et al. (2022) have estimated 1–7 MSPs, with four MSPs as the most likely, in NGC 6652. However, the background light curve matches the pulse phase bin of the lowest counts and the results from the phase-resolved analysis indicate that the major pulsed part contributes to most of the observed $\gamma$-ray emission from the GC, strongly suggesting small contributions from other sources. We note that the first MSP, J1835−3259A,

had no reported $\dot{P}$ (set to zero in DeCesar et al. 2015), which thus likely contributes little to the observed $\gamma$-ray emission. Paduano et al. (2021) reported a candidate transitional MSP (tMSP) in the GC, which has an X-ray luminosity of $1.8 \times 10^{34}$ erg s$^{-1}$. If this candidate is in a subluminous disk state or a pulsar state, its $\gamma$-ray luminosity would be $\sim 5 \times 10^{34}$ erg s$^{-1}$ ( i.e., $\sim L_{\gamma}$) or much higher respectively (based on the ratios of X-ray flux to $\gamma$-ray flux summarized for tMSPs in Miller et al. 2020). The $\gamma$-ray detection of J1835−3259B actually challenges the identification of the candidate tMSP. Thus it is very likely that the $\gamma$-ray emission from the GC comes dominantly from PSR J1835−3259B.

Intriguing questions remain to be investigated such as why, like NGC 6624 and NGC 6626, NGC 6652 also contains one exceptionally bright MSP. With $\gamma$-ray luminosities of $\sim$4–$9 \times 10^{34}$ erg s$^{-1}$, the three MSPs are among the brightest ones known (Wu et al. 2022). While the former two have higher spin-down luminosities of $\sim 10^{36}$ erg s$^{-1}$, these three all have relatively high rotational power among all MSPs. Also the former two are isolated pulsars, but PSR J1835−3259B is in a binary, likely with a helium white dwarf companion (Gautam et al. 2022), and on the evolutionary tracks for such binaries (Tauris & Savonije 1999). Further studies of pulsars in the GCs could help our understanding, by pinning down how many such bright MSPs exist in $\gamma$-ray-bright GCs.

We thank the anonymous referee for very helpful suggestions and W. Wu for inspiring this work and helping with the comparison of MSP properties. This work is supported in part by the National Key R&D Program of China under grant No. 2018YFA0404204, the National Natural Science Foundation of China No. 12163006, the Basic Research Program of Yunnan Province No. 202201AT070137, and the Foundations of Yunnan Province (202201BF070001-020). Z.W. acknowledges the support by the Original Innovation Program of the Chinese Academy of Sciences (E085021002) and the Basic Research Program of Yunnan Province No. 202201AS070005.

## ORCID iDs

Yi Xing https://orcid.org/0000-0002-5818-0732
Zhongxiang Wang https://orcid.org/0000-0003-1984-3852

## References

Abdo, A. A., Ackermann, M., Ajello, M., et al. 2009, Sci, 325, 845
Abdo, A. A., Ackermann, M., Ajello, M., et al. 2010a, A&A, 524, A75
Abdo, A. A., Ackermann, M., Ajello, M., et al. 2010b, ApJS, 188, 405
Abdo, A. A., Ajello, M., Allafort, A., et al. 2013, ApJS, 208, 17
Abdollahi, S., Acero, F., Ackermann, M., et al. 2020, ApJS, 247, 33
Atwood, W. B., Abdo, A. A., Ackermann, M., et al. 2009, ApJ, 697, 1071
Baumgardt, H., & Vasiliev, E. 2021, MNRAS, 505, 5957
Bhattacharya, D., & van den Heuvel, E. P. J. 1991, PhR, 203, 1
de Jager, O. C., & Büsching, I. 2010, A&A, 517, L9
de Menezes, R., Cafardo, F., & Nemmen, R. 2019, MNRAS, 486, 851
DeCesar, M. E., Ransom, S. M., Kaplan, D. L., Ray, P. S., & Geller, A. M. 2015, ApJ, 807, L23
Fermi-LAT Collaboration, Abdollahi, S., Acero, F., et al. 2022, ApJS, 260, 53
Freire, P. C. C., Abdo, A. A., Ajello, M., et al. 2011, Sci, 334, 1107
Gautam, T., Ridolfi, A., Freire, P. C. C., et al. 2022, A&A, 664, 54
Harris, W. E. 1996, AJ, 112, 1487
Hobbs, G., Edwards, R., & Manchester, R. 2006, ChJAS, 6, 189
Hui, C. Y., Cheng, K. S., Wang, Y., et al. 2011, ApJ, 726, 100
Johnson, T. J., Guillemot, L., Kerr, M., et al. 2013, ApJ, 778, 106
Kerr, M. 2011, ApJ, 732, 38
Kong, A. K. H., Hui, C. Y., & Cheng, K. S. 2010, ApJ, 712, L36
Lloyd, S. J., Chadwick, P. M., & Brown, A. M. 2018, MNRAS, 480, 4782
Manchester, R. N., Hobbs, G. B., Teoh, A., & Hobbs, M. 2005, AJ, 129, 1993
Miller, J. M., Swihart, S. J., Strader, J., et al. 2020, ApJ, 904, 49
Paduano, A., Bahramian, A., Miller-Jones, J. C. A., et al. 2021, MNRAS, 506, 4107
Ray, P. S., Kerr, M., Parent, D., et al. 2011, ApJS, 194, 17
Song, D., Macias, O., Horiuchi, S., Crocker, R. M., & Nataf, D. M. 2021, MNRAS, 507, 5161
Tam, P. H. T., Kong, A. K. H., Hui, C. Y., et al. 2011, ApJ, 729, 90
Tauris, T. M., & Savonije, G. J. 1999, A&A, 350, 928
Wu, J. H. K., Hui, C. Y., Wu, E. M. H., et al. 2013, ApJL, 765, L47
Wu, W., Wang, Z., Xing, Y., & Zhang, P. 2022, ApJ, 927, 117
Yuan, M., Zheng, J., Zhang, P., & Zhang, L. 2022, RAA, 22, 055019
Zhang, P. F., Xin, Y. L., Fu, L., et al. 2016, MNRAS, 459, 99
Zhang, P.-F., Zhou, J.-N., Yan, D.-H., et al. 2020, ApJL, 904, L29
Zhou, J. N., Zhang, P. F., Huang, X. Y., et al. 2015, MNRAS, 448, 3215